Prognostic Signature based on Transcriptome Characteristics of the C-C Motif Chemokine Receptor Genes in Hepatocellular Carcinoma and Validation

Xin Zhou
The First Affiliated Hospital of Guangxi Medical University
Ju-sen Nong
The First Affiliated Hospital of Guangxi Medical University
Tian-man Li
The First Affiliated Hospital of Guangxi Medical University
Zhong-liu Wei
The First Affiliated Hospital of Guangxi Medical University
Chen-lu Lan
The First Affiliated Hospital of Guangxi Medical University
Tian-hao Fu
The First Affiliated Hospital of Guangxi Medical University
Xi-wen Liao
The First Affiliated Hospital of Guangxi Medical University
Xin-ping Ye
The First Affiliated Hospital of Guangxi Medical University
Tao Peng (pengtaogmu@163.com)
The First Affiliated Hospital of Guangxi Medical University

Research Article

Keywords: hepatocellular carcinoma, C-C chemokine receptor, transcriptome, prognosis, immune infiltration

Posted Date: October 11th, 2021

DOI: https://doi.org/10.21203/rs.3.rs-882498/v1

Abstract

Object: This investigation aimed to assess the clinical significance of *C-C motif chemokine receptor* (*CCR*) genes in HCC and construct the prognostic signature based on transcriptome characteristics of the *CCRs*.

Methods: Clinical significance of *CCR*s were evaluated in TCGA database and GSE14520 dataset, and prognostic *CCRs* (*CCR1,5,7*) were screened out for validation and further analysis. The relationships between *CCR1,5,7* and prognosis were then evaluated in the Guangxi cohort. Based on the expression levels of *CCR1,5,7* and clinicopathological characteristics, the nomograms and prognostic signatures were respectively constructed in GSE14520 dataset and Guangxi cohort.

Results: *CCR1,5,7* were associated with overall survival of the HCC patients in GSE14520 database, TCGA database or Guangxi cohort. In the prognostic signature, the accuracy of prognosis risk assessment based on *CCR1,5,7* expression was satisfactory. The nomogram constructed in terms of the expression levels of *CCR1,5,7* and clinicopathological characteristics provided a convenient tool for clinician to assess the prognostic risk of each patient. GSEA results suggested that *CCRs* were mainly related to B cell receptor signal pathway, chemokine signaling pathway, T cell receptor signal pathway, etc. In addition, we also found that *CCR1,5,7* were significantly positively correlated with the degree of immune infiltration of B cells, T cells, and macrophages

Conclusion: *CCR1,5,7* might serve as prognostic biomarkers in HCC; *CCR1,5,7* might regulate the progression of HCC by impacting immune cells infiltration.

Introduction

There were 906,000 new cases of primary liver cancer worldwide in 2020, ranking sixth in the cancer incidence. Although liver cancer is the sixth most common malignant disease worldwide, it is the third cause of death related to malignant diseases[1,2]. Hepatocellular carcinoma (HCC) accounts for approximately 90% of all primary malignant tumors of the liver[3,4]. Cirrhosis of the liver, hepatitis B virus (HBV) and hepatitis C virus (HCV) infection, alcohol, nonalcoholic fatty liver disease (NAFLD), 2 diabetes and obesity are the risk factors for HCC[5,6]. It has brought huge suffering, decreased quality of life and a sharp reduction in survival time to patients, and at the same time caused a tremendous economic burden to the society. The situation of HCC in China is more severe. Among the malignant diseases, the incidence of HCC ranks fourth in China and the mortality of that ranks second[6,7]. In some regions of China, such as Guangxi, due to high exposure to hepatitis B and aflatoxin, the incidence and mortality of hepatocellular carcinoma has been the first among local malignancies for four decades[7]. The Tyrosine Kinase Inhibitor (TKI) represented by Sorafenib and Lenvatinib did extend survival in some HCC patients, but the overall therapeutic effect was not satisfactory[8,9]. Immune checkpoint inhibitors (ICI) also didn't work well in hepatocellular carcinoma alone[10,11]. The results of clinical studies in the past two years, regarding the combination of TKI and ICI, seem to offer hope for patients with advanced liver cancer[12]. The median progression-free survival (PFS) of patients taking Lenvatinib and Pabrizumab together has reached 9.7 months, and 6-month and 12-month survival rates were 83.3% and 59.8%, respectively[13]. The results of the program were considered groundbreaking. Although breakthroughs have been made in the treatment of HCC, for now, we still have a long way to go.

Chemokine receptors are known for their biological roles in chemotaxis, target cell migration, and inflammation[14]. They are not only indispensable for all protective or destructive immune and inflammatory activities, but also play an important role in the development and homeostasis of the human immune system[15,16]. Because of their important role, chemokines are closely associated with multiple diseases, such as cancer, viral infections, inflammation, and autoimmune diseases. In recent decades, chemokine system has considered as potential target for immunotherapy[17,18]. Chemokines are a large class of chemotactic cytokines, whose homologous receptors, chemokines receptors, are expressed in both tumor cells and stromal cells[19]. Given that chemokine receptors are involved in multiple aspects of cancer biology, their potential targets have been assessed in many preclinical studies and clinical trials. Monoclonal antibodies (anti-CCR4 mAb, Mogamulizumab) and chemokine receptor inhibitors (CXCR4 antagonist AMD3100) are already being applied for hematologic malignancies in clinical[20,21]. The chemokine receptors have been grouped to subfamilies - CCR, CXCR, XCR and CX3CR – in terms of cysteine motif variations. The purpose of this investigation is to inspect the role of CCR subfamily members in HCC.

Materials And Methods

Function annotation and pathway enrichment of CCR genes

Function annotation for *CCRs* (*CCR* genes) in terms of gene ontology (GO) and KEGG pathway was performed on Database for Annotation, Visualization and Integrated Discovery (DAVID) v6.8[22,23]. Function annotation clustering results were then visualized in R studio with packages GOplot[24], Hmisc[25], and ggplot2[26].

Data sources and tissue specimen collection

Transcriptome sequencing data of 212 HCC patients and corresponding prognostic data in GSE14520 were obtained from GEO database[27], with 8 patients' para-carcinoma tissues of missing. Transcriptome sequencing data of 370 HCC tissues and 50 para-carcinoma tissues were downloaded from TCGA database. In the first affiliated hospital of Guangxi Medical University, fresh liver tissues (HCC and para-carcinoma tissues) of 25 HCC patients were collected and then immersed in RNAstore Reagent (TIANGEN, Beijing). Tissue specimens were stored in the -80°C refrigerator. All patient had signed the informed consent for investigation before operation. The study had been approved by the ethics committee of Guangxi Medical University the first affiliated hospital (Approval number: 2015 [KY-E-032]).

Expression difference analysis, correlation analysis and diagnostic efficiency

Student's t test was used to analyze the expression difference of *CCRs* between HCC tumor tissues and para-carcinoma tissues. $P<0.05$ was considered statistically significant in Student's t test. The correlation coefficient of *CCRs* expression in HCC tissues was calculated in R with *corrplot* package. ROC (receiver operating characteristic curve) was used for assess the diagnostic efficiency of *CCRs*. The Area Under Curve (AUC) of the ROC curve exceed 0.70 was considered to be with satisfactory diagnostic efficacy.

Survival analysis

In GSE14520, Kaplan-Meier method and Cox proportional hazards model were respectively used for survival analysis of HCC patients in terms of expression of *CCRs*. Bias of clinical characteristics for survival were adjusted in Cox proportional hazards model. The *CCRs* associated with the OS of HCC patients in GSE14520 were integrated for combined effect survival analysis. Patients were assigned to groups based on the expression levels of multiple *CCRs*. Kaplan-Meier Plotter (https://kmplot.com/) is an online survival analysis website which has integrated several databases[28]. It was used to further inspect the prognostic significance of *CCRs* in TCGA database. Kaplan-Meier method was also applied for survival analysis in Guangxi cohort.

Nomogram

The nomogram was constructed in R studio with *foreign* package (Version 1.2.5033, R 3.6.2) in terms of clinical characteristics and expression of *CCRs*. Multiple value levels of each influencing factor are assigned points, and the total score is obtained by adding the scores of each influencing factor. The prediction probability of the individual's outcome event is calculated through the function transformation relationship between the total score and the occurrence probability of the terminal event. Bootstrap self-sampling method was used to verify the prediction efficiency of the nomogram.

Prognostic signature construction

Prognostic signature was constructed with the expression of *CCRs* and prognostic data. According to the regression coefficients and expression value of *CCRs*, risk score for each HCC patient was calculated: risk score = expression value of $gene_1$ x β_1+ expression value of $gene_2$ x β_2 +…+ expression value of $gene_n$ x β_n, where β was the regression coefficient derived from the multivariate Cox proportional hazards regression model. Kaplan-Meier method was used to compare the outcome between high and low risk score groups. Time-dependent ROC curve was structured with the *survivalROC* package in R studio (Version 1.2.5033, R 3.6.2) to further evaluate the prediction efficiency.

Quantitative polymerase chain reaction (qPCR)

Total RNA was extracted from Fresh tissues (HCC and para-carcinoma tissues) of 25 HCC patients and reversed transcribed into complementary DNA. qPCR was used to quantitatively analyze the expression of *CCR1*, *CCR5* and *CCR7* with Fast Start Universal SYBR Green Master (Roche, Germany). Primers for *CCR1*, *CCR5* and *CCR7* and *GAPDH* (reference gene) were synthesized by Sangon Biotech Company. The forward and reverse primer sequences of *CCR1*, *CCR5* and *CCR7* and *GAPDH* were as follows:

GAPDH: forward 5'-TCAGCCGCATCTTCTTT-3'

reverse 5'-CGCCCAATACGACCAAAT-3'

CCR1: forward 5'-CTGTGTCAACCCAGTGATCTAC-3'

reverse 5'-GAGGAAGGGGAGCCATTTAAC-3'

CCR5: forward 5'-GCAGCTCTCATTTTCCATACAG-3'

reverse 5'-GACACCGAAGCAGAGTTTTTAG-3'

CCR7: forward 5'-CATGCTCCTACTTCTTTGCATC-3'

reverse 5'-CACTGTGGCTAGTATCCAGATG-3'

Immunohistochemistry (IHC)

The tissue sections of 25 patients were obtained from the Department of Pathology, the First Affiliated Hospital of Guangxi Medical University. IHC assay was performed with the Universal two-step IHC kit (PV-9000, ZSGB-BIO, Biotech, Beijing) according to the manufacturer's protocol. The primary antibodies against CCR1(DF2710, Affinity, Jiangsu, China), CCR5 (AF6339, Affinity, Jiangsu, China) and CCR7 (AF5293, Affinity, Jiangsu, China) and peroxidase-conjugated goat antirat IgG (ZB-2307, ZSGB-BIO, Beijing, China) were used in the IHC assay. Sections were incubated overnight with primary antibody at 4 °C. The primary antibody titer was configured according to the manufacturer's recommended IHC concentration (CCR1, 1:200; CCR5, 1:300; CCR7, 1:100).

Gene set enrichment analysis (GSEA)

According to the median of *CCR* expression, the HCC patients in GSE14520/TCGA were divided into high and low expression *CCR* groups for GSEA. GSEA was used to explore whether there were statistical differences in Molecular Signatures Database (MSigDB) c2(c2.all.v7.0.symbols.gmt) between the genomes of high and low expression groups[29], by virtue of standardized enrichment scores and false detection rates as criteria for determining statistical significance. The significance threshold is set to P<0.05 and false discovery rate (FDR) <0.25.

Tumor-Infiltrating Immune Cells

TIMER is A Web Server for Comprehensive Analysis of Tumor-Infiltrating Immune Cells[30]. It was applied for inspect the correlation between *CCR* genes and tumor-infiltrating immune cells in this investigation. We mainly explored the correlation between *CCRs* and B cells, $CD8^+$ T cell, $CD4^+$ T cell and macrophage. Correlation coefficient was used to evaluate the correlation between the expression level and the degree of cell invasion. The significance threshold is set to Correlation coefficient>0.300 and *P*<0.05

Statistical analysis

Student's T test was used for compare the expression difference between HCC group and para-carcinoma group. Kaplan Meier method with Log-rank test and Cox proportional hazards model was respectively applied for survival analysis. ROC analysis was performed for assessing diagnostic efficiency. Statistical calculation was implemented in SPSS 22.0 or R studio (Version 1.2.5033, R 3.6.2) except GSEA. GSEA was accomplished in software GSEA v4.0.3. Statistical significance was achieved when *P*<0.05 in Student's t test, ROC, Log-rank test and Cox proportional hazards model. The hazard ratio was shown with a 95% confidence interval.

Results

Function annotation and pathway enrichment result of CCR genes.

It was revealed in the gene functional enrichment analysis that CCR genes was enriched in chemotaxis, positive regulation of cytosolic calcium ion concentration, chemokine-mediated signaling pathway, immune response, dendritic cell chemotaxis, cellular defense response, and so on (figure 1A). The correspondence between *CCRs* and GO terms was shown in figure 1B. The details of the enriched Gene Ontology (GO) terms in molecular function (MF), biological process (BP) and cellular component (CC) categories and KEGG pathway for CCR genes was displayed in table S1.

Expression of *CCRs* in HCC and para-carcinoma tissues

It was observed in GSE14520 cohort that expression of *CCR1*, *CCR2*, *CCR3*, *CCR5*, *CCR7* and *CCR8* in HCC tissues were significantly lower than para-carcinoma tissues, whereas expression of *CCR6* and *CCR9* was higher in HCC tissues (figure 2A). CCR4 and CCR10 are the only two members of the CCR family that show no difference in expression between HCC and para-carcinoma tissues. Expression correlation analysis between any two members of the CCR family showed that there were strong correlations among expression of *CCR1*, *CCR2*, *CCR5*, and *CCR7* in HCC (figure 2B).

Then, we further evaluated the expression characteristics of CCR family genes in HCC in TCGA cohort. It was observed that expression of *CCR1*, *CCR2*, *CCR4*, *CCR5*, *CCR7* and *CCR9* were significantly lower in HCC tissues, whereas expression of *CCR3*, *CCR8* and *CCR10* were significantly higher in HCC tissues (figure 2C). Expression correlation analysis indicated that there were relatively high expression correlations among *CCR1*, *CCR2*, *CCR4*, *CCR5*, *CCR6, CCR7* and *CCR8* in HCC (figure 2D).

Diagnostic significance of CCRs in HCC

After a preliminary exploration of the expression characteristics of CCR gene family members in HCC, we assessed the possibility of these genes as diagnostic markers of HCC using the area under the ROC curve. In GSE14520 cohort, *CCR1* (AUC=0.731, figure 3A) and *CCR5* (AUC=0.714, figure 3E) was observed to be with good diagnostic performance in HCC, while diagnostic significance of the other CCR family members (figure 3B-D, F-J) were not satisfactory. In TCGA cohort, *CCR1* (AUC=0.833, figure 3K) and *CCR9* (AUC=0.835, figure 3S) was found to be with good diagnostic performance in HCC, while diagnostic significance of the other CCR family members (figure 3L-R, T) were not satisfactory.

Survival analysis result in GSE14520 and TCGA

In addition to whole-transcriptome microarray data and prognostic data, clinical information on 212 HCC patients was obtained from the GSE14520 dataset. In order to adjust for the effect of clinical factors in subsequent survival analyses, we first investigated the relationship between clinical factors and prognosis. The baseline information about the 212 HCC patients was displayed in table S2. It revealed that tumor size, cirrhosis, BCLC stage, TNM stage and AFP were associated with the OS of HCC, and tumor size, gender, TNM stage and BCLC stage were associated with the RFS of HCC.

We analyzed the relationship between CCR family members and RFS in GSE14520 and TCGA, respectively. In GSE14520 cohort, none of *CCR* gene was observed to be associated with RFS of patients in HCC, neither in univariate survival analysis nor after adjustment for clinical factors in Cox proportional hazards model (table 1, figure 4A-J); However, In TCGA cohort, *CCR1*, *CCR2*, *CCR4*, *CCR5*, *CCR6*, *CCR7*, *CCR8* and *CCR9* were observed to be associated with RFS of patients in HCC (figure 4K, L, N-S), while prognostic significance was not found for *CCR3*, *CCR10* (figure 4M, T).

Then we evaluated the relationship between CCR family members and OS in GSE14520 and TCGA, respectively. Prognostic significance of *CCR1* in OS (*P*=0.189, table 1, figure 5A) was not observed in univariate survival analysis; however, it (adjusted *P*=0.044, table 1) was observed to be associated with OS in Cox proportional hazards model after adjusted for clinical factors. *CCR5* (*P*=0.022, adjusted *P*=0.021, table 1, figure 5E) and *CCR7* (*P*=0.021, adjusted *P*=0.039, table 1, figure 5G) were both significantly correlated with OS in either Cox proportional hazards model or Kaplan Meier method in GSE14520 cohort. Other members of the CCR gene family were found to be associated with OS in HCC (figure 5B-D, F, H-J).

In TCGA cohort, *CCR1*, *CCR2*, *CCR3*, *CCR4*, *CCR5* and *CCR7* were observed to be associated with OS (figure 5K-O, Q), while prognostic significance for *CCR6*, *CCR8*, *CCR9* and *CCR10* were not observed (figure 5P, R-T).

Nomogram and prognostic signature

Based on the prognostic significance of CCR1, CCR5 and CCR7 found in our above study, in order to optimize our discovery and produce a better predictive prognostic model for patients with HCC, we respectively performed combined effect survival analysis, nomogram and prognostic signature in terms of the data of GSE14520. Combined analysis of *CCR1* and *CCR5* in HCC showed that patients in the group with low expression of *CCR1* and *CCR5* had the best outcome (figure 6A). Similarly, in other combined analyses, the patient in the group □, the patients in the group c and the patients in group 3 all had the longest survival in their respective comparisons (figure 6B-D). The grouping protocols and outcomes were listed in table 2. We observed that the differences between the best and worst groups were more significant in the combined analysis than in the single gene survival analysis.

We established a nomogram and a prognosis signature based on the expression levels of *CCR1*, *CCR5* and *CCR7* in GSE14520. In nomogram, the length of corresponding line segment of each variable represents its contribution degree for prognosis. The parameter with the highest prognostic contribution was BCLC stage, followed by the degree of cirrhosis. The contribution of *CCR1*, *CCR5* and *CCR7* in predicting prognosis were similar (figure 6E). We evaluated the predictive power of the histogram by the match degree between the training group and the validation group. In the nomogram of GSE14520, there was a high degree of superposition between the self-validation cohort (red line) and training group (gray line) for predicting a 1-, 3 -, or 5-year prognosis (figure 6F-H).

The risk score formula for prognosis signature in GSE14520 was: risk score = expression value of *CCR1* x -0.278 + expression value of *CCR5* x -0.348 + expression value of *CCR7* x -0.306. A total of 212 patients with HCC in GSE14520 were classified as high-risk group or low-risk group. Ranking patients by risk score from left to right (figure 6I, K), we observed that patients in the high-risk group had a higher concentration of individuals who reach terminal event in short term (figure 6J). The difference between the high and low risk groups in OS was statistically significant (*P*=0.025, figure 6L). Besides, the ROC curve also revealed that the prognostic signature worked well in predicting 1-, 2-, 3-, 4-, and 5-year outcome (figure 6M).

Validation for clinic significance of CCR1,5,7 in Guangxi cohort

Twenty-five patients from the Department of Hepatobiliary Surgery of Guangxi Medical University were enrolled as a validation cohort. The baseline data of the HCC patients in Guangxi cohort are listed in Table S3. In Guangxi cohort, IHC assay and qPCR assay showed that *CCR1*, *CCR5* and *CCR7* expression were significantly decreased in HCC tissues (figure 7A, B). Meanwhile, we observed that the expression levels of *CCR1*, *CCR5* and *CCR7* were strongly correlated (figure 7C). Besides, it was observed in Guangxi cohort that *CCR1*, *CCR5* and *CCR7* performed well in HCC diagnosis (figure 7D-F). In full agreement with the results in GSE14520 and TCGA database, *CCR1* (*P*=0.045, table 3, figure 7G), *CCR5* (*P*=0.013, table 3, figure 7H) and *CCR7* (*P*=0.029, table 3, figure 7I) were significantly associated with prognosis of HCC, and their up-regulated expression predicting a good prognosis.

Nomogram and Prognostic signature construction in Guangxi cohort.

Based on the expression of *CCR1*, *CCR5* and *CCR7*, we constructed the prognostic signature and the nomogram for HCC patients of Guangxi cohort. The risk score formula in Guangxi cohort was: risk score = expression value of *CCR1* x -0.845 + expression value of *CCR5* x -0.117 + expression value of *CCR7* x -0.129. The risk score and the time of outcome event in HCC patients of Guangxi cohort of were displayed in the scatter plots (figure 8A, B), and the *CCR1*, *CCR5* and *CCR7* expression profile of these patients was shown using heat map. We observed that patients in the high-risk group had a shorter survival compared to those in the low-risk group. The results of survival analysis in the high and low risk groups indicated that the difference in prognosis was statistically significant (figure 8D, *P*=0.006). the survival ROC curve indicated that the prognostic signature worked well in predicting 1 year OS (figure 8E).

In the nomogram constructed in Guangxi cohort, the parameter with the highest prognostic contribution was tumor size, followed by the AFP (figure 8F). Predictive power of the nomogram was assessed using the match degree between the training group and the validation group. In the nomogram of Guangxi cohort, there was a high degree of superposition between the self-validation cohort (red line) and training group (gray line) for predicting a 1- or 2-year prognosis (figure 8G-H).

GSEA

After intersecting the GSEA result of GSE14520 cohort with the GSEA result of TCGA cohort, it was observed that the results of these two datasets were very similar. Some of the more representative results were presented. It revealed that *CCR1* (figure 9A, B) was associated with B cell receptor signal pathway, chemokine signaling pathway, nod-like receptor signal pathway, T cell receptor signal pathway, JAK-STAT signaling pathway, etc. *CCR5* (figure 9C, D) was associated with B cell receptor signal pathway, chemokine signaling pathway, cytokine- cytokine receptor signal pathway, T cell receptor signal pathway, toll-like receptor signaling pathway, etc. *CCR7* (figure 9E, F) was associated with B cell receptor signal pathway, chemokine signaling pathway, natural killer mediated cytotoxicity, nod-like receptor signal pathway, toll-like receptor signaling pathway, etc. We observed that these *CCR* genes were enriched in very similar pathways in HCC data sets, which suggested that there might be synergy between them.

Tumor-Infiltrating Immune Cells

We found a significant association between CCR1,5,7 and immune cell infiltration. *CCR1* was positively correlated with the degree of B cells (Cor=0.498), $CD8^+$ T cell (Cor=0.500), $CD4^+$ T cell (Cor=0.389) and macrophage (Cor=0.629) infiltration in HCC tissues (figure 10A). *CCR5* was also positively correlated with the degree of B cells (Cor=0.634), $CD8^+$ T cell (Cor=0.680), $CD4^+$ T cell (Cor=0.477) and macrophage (Cor=0.552) infiltration in HCC tissues (figure 10B). Similarly, the HCC tissues with high expression of CCR7 was companied with high degree infiltration of B cells (Cor=0.456), $CD8^+$ T cell (Cor=0.405), $CD4^+$ T cell (Cor=0.429) and macrophage (Cor=0.302) (figure 10C).

Discussion

Due to its high incidence and fatality rate, HCC brings great suffering to patients. Early screening and prognostic biomarkers for HCC are urgently needed, which may bring hope for the prevention and treatment of HCC. In recent years, the achievements of immune research have brought a breakthrough in the treatment of HCC. As chemokine receptors, *CCRs* play important roles in immunity and inflammation, but there are few reports on *CCRs* in HCC. In this investigation, we inspected the clinical significance of members of the CCR gene family in multiple datasets, and further explored the possible mechanisms of CCR gene in HCC via bioinformatics tools.

We first explored genes that are differentially expressed in HCC and para-carcinoma tissue. The differentially expressed genes in TCGA LIHC dataset and GSE14520 dataset were not completely coincident, possibly due to ethnic inconsistency between the two datasets. Hepatocellular carcinoma patients in GSE14520 were all from China, represented by the yellow race, while HCC patients in the TCGA data set were mainly Caucasian. Even so, we found some common ground from the results of the two datasets. we observed that *CCR1*, *CCR2*, *CCR5* and *CCR7* were significantly lower expressed in HCC tissues in TCGA LIHC dataset and GSE14520 dataset, compared with para-carcinoma tissues.

Furthermore, survival analysis in TCGA and GSE14520 showed that *CCR1*, *CCR2*, and *CCR7* were all significantly associated with OS of HCC patients. Integral analysis, nomogram, and prognostic model in terms of *CCR1*, *CCR2*, and *CCR7* All showed good performance in prognosis evaluation of HCC. It should be noted that high expression of CCR1 in GSE14520 was associated with good outcome, whereas high expression of CCR1 in TCGA was associated with poor prognosis. We further examined the prognostic significance of *CCR1*, *CCR5* and *CCR7* in patients with HCC in Guangxi. We get exactly the same tendency as the GSE14520 dataset. Hepatitis B virus exposure is the main cause of HCC in China, while NAFLD is the main cause of HCC in the United States of America. We hypothesized that *CCR1* might play distinct roles in HCC with different pathogeny backgrounds.

We reviewed some reports on *CCR1* in multiple cancers. It prompted that higher expression of CCR1 was correlated to better prognosis of head and neck cancer, ovarian cancer and melanoma[31]. Whereas some other report showed that higher expression of CCR1 was accompanied with worse outcome of glioma, lung cancer, renal cancer, testicular cancer[32]. Zhu M et al. found that CCL14 could Induce apoptosis of hepatocellular carcinoma cells by activating CCR1[33]. This report supported our conclusion in the GSE14520 and Guangxi cohorts. It has also been found that CCL15 induces HCC cell migration and invasion through activation of CCR1, leading to a worse prognosis[34]. Besides. CCL15 also induces CCR1 /CCR3-mediated angiogenesis on vascular endothelial cells[35]; CCL16 also could promote angiogenesis of HCC via CCR1 activation[36]. There reports confirmed our findings in the TCGA database. CCR1 has many ligands, including CCL2, CCL3, CCL4, CCL5, CCL7, CCL8, CCL14, CCL15, CCL16, and CCL23. The levels of chemokines are different among people with different backgrounds of HCC, and then resulting in radically different consequences, via CCR1 activation.

CCR5 was usually acknowledged as the HIV specific binding site in T cell surface. Accompanied with the rise of immunotherapy, we begun to notice the role of CCR5 in tumors. CCR5 expression has reported to be associated with the growth of multiple cancers, including breast cancer, ovarian cancer, cervical cancer, prostate cancer, colon cancer, melanoma, Hodgkin's lymphoma, and multiple myeloma[37]. XW Wang et al. found that activation of the CCL4/CCR5 axis significantly induced γδ T-cells infiltration in HCC, thereby improving prognosis of HCC. Leronlimab (PRO140) is a humanized IgG4 monoclonal antibody that targets chemokine receptor 5 (CCR5). In cell and animal models, it has been demonstrated to block tumor metastasis in invasive breast and prostate cancers[38]. Although the function of CCR5 in HCC is still unknown, the CCR5/CCL5 axis was attested to be associated with chronic liver inflammation caused by a variety of pathogens and be involved in the occurrence and development of HCC[39,40]. The Human Protein Atlas (https://www.proteinatlas.org/) shown that patients with upregulated CCR5 have better outcomes in a number of cancers, including thyroid, lung, colorectal, head and neck, stomach, liver, prostate, breast and cervical cancers; However, CCR5 was found to be associated with a poor prognosis in several cancers, such as Glioma, kidney cancer and Testis cancer[31,32].The prognosis of CCR5 in multiple cancers seems to validate the function of CCR5 in this investigation.

Hypoxia and prostaglandin E2 increase the expression level of CCR7 on cancer cells, thereby affecting cell stemness and proliferation potential[15,41–45]. In colorectal cancer cells, CCL19 activates CCR7, thereby inducing miR-206 upregulation to suppress angiogenesis, with miR-206 upregulation inhibiting ERK/MAPK-HIF-1-VEGF pathway[46]. This study was the first to inspect the prognostic significance of CCR7 in HCC in multiple data sets and reach consistent conclusions. CCR7 was found to be strongly associated with better outcomes in patients with hepatocellular carcinoma.

GSEA results of *CCR1*, *CCR5*, and *CCR7* were very similar, and all three were found to be related to the chemotactic function of B cells and T cells. Subsequently, we investigated the correlation between *CCR1*, *CCR5*, and *CCR7* and the degree of immune cell infiltration in the tumor microenvironment. The results are consistent with the GSEA discovery. We observed that *CCR1*, *CCR5*, and *CCR7* were positively correlated with the degree of B cells, CD8+ T cell, CD4+ T cell and macrophage infiltration in HCC tissues.

There were several limitations in this investigation. The sample size of Guangxi cohort in this investigation was small, and a larger sample size might make the results more reliable. This study preliminarily discussed the diagnostic and prognostic value of *CCR* genes in HCC, however, the function of diagnostic and prognostic biomarkers in HCC still needs to be further verified by experiments. We found that *CCR1*,*5,7* were related to B cells, CD8+ T cell, CD4+ T cell and macrophage infiltration in HCC tissues. However, the mechanism of leukocyte enrichment caused by them is still unclear, and animal experiments may be needed to clarify it.

Conclusion

It was discovered that *CCR1*,*5,7* were associated with OS of patients in HCC. *CCRs* were closely relevant to B cell receptor signal pathway, chemokine signaling pathway, T cell receptor signal pathway, etc. In addition, we also found that *CCR1*,*5,7* were significantly positively correlated with the degree of immune infiltration of B cells, $CD8^+$ T cell, $CD4^+$ T cell and macrophage. We suspected that *CCR1*,*5,7* were crucial prognostic biomarkers in HCC, and *CCR1*,*5,7* might impact HCC by induce immune cells infiltration.

Abbreviations

CCR: C-C motif chemokine receptor

GSEA: Gene Set Enrichment Analysis

HCC: Hepatocellular Carcinoma

HBV: Hepatitis B Virus

NAFLD: Non-alcohol Fatty Liver Disease

HCV: Hepatitis C virus

DAVID: Database for Annotation, Visualization and Integrated Discovery

GO: Gene ontology

ROC: receiver operating characteristic curve

AUC: The Area Under Curve

qPCR: Quantitative polymerase chain reaction

IHC: Immunohistochemistry

Declarations

Ethics approval and consent to participate

All patient in the Guangxi cohort had signed the informed consent. The investigation had been approved by the ethics committee of Guangxi Medical University the first affiliated hospital (Approval number: 2015 [KY-E-032]). All methods in this research were carried out in accordance with Declaration of Helsinki.

Consent for publication

Not Applicable.

Availability of data and material

The datasets used and/or analyzed during the current study are available from the corresponding author on reasonable request

Competing interests

Not Applicable.

Funding

This research was partly supported by professor Tao Peng with Key Laboratory of early Prevention & Treatment for regional High Frequency Tumor (Guangxi Medical University)-Ministry of Education (grant nos. GKE2018-01, GKE2019-11 and GKE-ZZ202009). Besides, it was also supported by professor Xin-ping Ye with Guangxi Key Laboratory for the Prevention and Control of Viral Hepatitis (No. GXCDCKL201902) and Natural Science Foundation of Guangxi Province of China (grant no. 2020GXNSFAA159127).

Authors' contributions

X Zand J N conceived and designed the manuscript; Z W, J N, C L and J L made acquisition of data; T F and X L performed data analysis. RNA extraction and qPCR were done by T L and X L. X Z wrote the manuscript, and T p and X Y guided and supervised the manuscript. All authors read and approved the final manuscript. All authors made a significant contribution to the work reported, whether that is in the conception, study design, execution, acquisition of data, analysis and interpretation, or in all these areas; took part in drafting, revising or critically reviewing the article; gave final approval of the version to be published; have agreed on the journal to which the article has been submitted; and agree to be accountable for all aspects of the work.

Acknowledgements

The authors thank the contributors of GSE14520 and TCGA database for sharing the HCC dataset on open access.

References

1. Bray F, Ferlay J, Soerjomataram I, Siegel RL, Torre LA, Jemal A. Global cancer statistics 2018: GLOBOCAN estimates of incidence and mortality worldwide for 36 cancers in 185 countries. *CA Cancer J Clin.* 2018;68(6):394–424.
2. Sung H, Ferlay J, Siegel RL, et al. Global cancer statistics 2020: GLOBOCAN estimates of incidence and mortality worldwide for 36 cancers in 185 countries. *CA Cancer J Clin*. 2021.
3. Villanueva A. Hepatocellular Carcinoma. *N Engl J Med.* 2019;380(15):1450–1462.
4. Siegel RL, Miller KD, Jemal A. Cancer statistics, 2020. *CA Cancer J Clin.* 2020;70(1):7–30.
5. Kulik L, El-Serag HB. Epidemiology and Management of Hepatocellular Carcinoma. *Gastroenterology.* 2019;156(2):477-491 e471.
6. Chen W, Zheng R, Baade PD, et al. Cancer statistics in China, 2015. *CA Cancer J Clin.* 2016;66(2):115–132.
7. Zhang CY, Huang TR, Yu JH, et al. Epidemiological analysis of primary liver cancer in the early 21st century in Guangxi province of China. *Chin J Cancer.* 2010;29(5):545–550.
8. Keating GM. Sorafenib: A Review in Hepatocellular Carcinoma. *Target Oncol.* 2017;12(2):243–253.
9. Keating GM, Santoro A. Sorafenib: a review of its use in advanced hepatocellular carcinoma. *Drugs.* 2009;69(2):223–240.
10. Abd El Aziz MA, Facciorusso A, Nayfeh T, et al. Immune Checkpoint Inhibitors for Unresectable Hepatocellular Carcinoma. *Vaccines (Basel)*. 2020;8(4).
11. Federico P, Petrillo A, Giordano P, et al. Immune Checkpoint Inhibitors in Hepatocellular Carcinoma: Current Status and Novel Perspectives. *Cancers (Basel).* 2020;12(10).
12. Kalasekar SM, Garrido-Laguna I, Evason KJ. Immune Checkpoint Inhibitors in Novel Combinations for Hepatocellular Carcinoma. *Hepatology.* 2021.
13. Kudo M, Finn RS, Qin S, et al. Lenvatinib versus sorafenib in first-line treatment of patients with unresectable hepatocellular carcinoma: a randomised phase 3 non-inferiority trial. *Lancet.* 2018;391(10126):1163–1173.
14. Stuart MJ, Baune BT. Chemokines and chemokine receptors in mood disorders, schizophrenia, and cognitive impairment: a systematic review of biomarker studies. *Neurosci Biobehav Rev.* 2014;42:93–115.
15. Lopez-Cotarelo P, Gomez-Moreira C, Criado-Garcia O, Sanchez L, Rodriguez-Fernandez JL. Beyond Chemoattraction: Multifunctionality of Chemokine Receptors in Leukocytes. *Trends Immunol.* 2017;38(12):927–941.
16. Charo IF, Ransohoff RM. The many roles of chemokines and chemokine receptors in inflammation. *N Engl J Med.* 2006;354(6):610–621.
17. Lokeshwar BL, Kallifatidis G, Hoy JJ. Atypical chemokine receptors in tumor cell growth and metastasis. *Adv Cancer Res.* 2020;145:1–27.
18. Miller MC, Mayo KH. Chemokines from a Structural Perspective. *Int J Mol Sci.* 2017;18(10).
19. van der Vorst EP, Doring Y, Weber C. Chemokines. *Arterioscler Thromb Vasc Biol.* 2015;35(11):e52-56.
20. Moore DC, Elmes JB, Shibu PA, Larck C, Park SI. Mogamulizumab: An Anti-CC Chemokine Receptor 4 Antibody for T-Cell Lymphomas. *Ann Pharmacother.* 2020;54(4):371–379.
21. Wang J, Tannous BA, Poznansky MC, Chen H. CXCR4 antagonist AMD3100 (plerixafor): From an impurity to a therapeutic agent. *Pharmacol Res.* 2020;159:105010.
22. Huang DW, Sherman BT, Lempicki RA. Systematic and integrative analysis of large gene lists using DAVID bioinformatics resources. *Nat Protoc.* 2009;4(1):44–57.
23. Huang DW, Sherman BT, Lempicki RA. Bioinformatics enrichment tools: paths toward the comprehensive functional analysis of large gene lists. *Nucleic Acids Res.* 2009;37(1).

24. Nolan DJ, Ginsberg M, Israely E, et al. Molecular signatures of tissue-specific microvascular endothelial cell heterogeneity in organ maintenance and regeneration. *Dev Cell.* 2013;26(2):204–219.
25. Liu K, Feng F, Chen X-Z, et al. Comparison between gastric and esophageal classification system among adenocarcinomas of esophagogastric junction according to AJCC 8th edition: a retrospective observational study from two high-volume institutions in China. *Gastric Cancer.* 2019;22(3):506–517.
26. Ito K, Murphy D. Application of ggplot2 to Pharmacometric Graphics. *CPT Pharmacometrics Syst Pharmacol.* 2013;2:e79.
27. Roessler S, Jia HL, Budhu A, et al. A unique metastasis gene signature enables prediction of tumor relapse in early-stage hepatocellular carcinoma patients. *Cancer Res.* 2010;70(24):10202–10212.
28. Nagy Á, Lánczky A, Menyhárt O, Győrffy B. Validation of miRNA prognostic power in hepatocellular carcinoma using expression data of independent datasets. *Scientific reports.* 2018;8(1):9227.
29. Subramanian A, Kuehn H, Gould J, Tamayo P, Mesirov JP. GSEA-P: a desktop application for Gene Set Enrichment Analysis. *Bioinformatics.* 2007;23(23):3251–3253.
30. Li T, Fan J, Wang B, et al. TIMER: A Web Server for Comprehensive Analysis of Tumor-Infiltrating Immune Cells. *Cancer Res.* 2017;77(21):e108-e110.
31. Uhlen M, Fagerberg L, Hallstrom BM, et al. Proteomics. Tissue-based map of the human proteome. *Science.* 2015;347(6220):1260419.
32. Uhlen M, Zhang C, Lee S, et al. A pathology atlas of the human cancer transcriptome. *Science.* 2017;357(6352).
33. Zhu M, Xu W, Wei C, et al. CCL14 serves as a novel prognostic factor and tumor suppressor of HCC by modulating cell cycle and promoting apoptosis. *Cell Death Dis.* 2019;10(11):796.
34. Li Y, Yu HP, Zhang P. CCL15 overexpression predicts poor prognosis for hepatocellular carcinoma. *Hepatol Int.* 2016;10(3):488–492.
35. Hwang J, Kim CW, Son KN, et al. Angiogenic activity of human CC chemokine CCL15 in vitro and in vivo. *FEBS Lett.* 2004;570(1-3):47–51.
36. Strasly M, Doronzo G, Cappello P, et al. CCL16 activates an angiogenic program in vascular endothelial cells. *Blood.* 2004;103(1):40–49.
37. Aldinucci D, Colombatti A. The inflammatory chemokine CCL5 and cancer progression. *Mediators Inflamm.* 2014;2014:292376.
38. Jiao X, Nawab O, Patel T, et al. Recent Advances Targeting CCR5 for Cancer and Its Role in Immuno-Oncology. *Cancer Res.* 2019;79(19):4801–4807.
39. Lin YL, Liu CC, Chuang JI, et al. Involvement of oxidative stress, NF-IL-6, and RANTES expression in dengue-2-virus-infected human liver cells. *Virology.* 2000;276(1):114–126.
40. Nahon P, Sutton A, Rufat P, et al. Chemokine system polymorphisms, survival and hepatocellular carcinoma occurrence in patients with hepatitis C virus-related cirrhosis. *World J Gastroenterol.* 2008;14(5):713–719.
41. Li Y, Qiu X, Zhang S, Zhang Q, Wang E. Hypoxia induced CCR7 expression via HIF-1alpha and HIF-2alpha correlates with migration and invasion in lung cancer cells. *Cancer Biol Ther.* 2009;8(4):322–330.
42. Chuang CW, Pan MR, Hou MF, Hung WC. Cyclooxygenase-2 up-regulates CCR7 expression via AKT-mediated phosphorylation and activation of Sp1 in breast cancer cells. *J Cell Physiol.* 2013;228(2):341–348.
43. Pan MR, Hou MF, Chang HC, Hung WC. Cyclooxygenase-2 up-regulates CCR7 via EP2/EP4 receptor signaling pathways to enhance lymphatic invasion of breast cancer cells. *J Biol Chem.* 2008;283(17):11155–11163.
44. Cheng S, Han L, Guo J, Yang Q, Zhou J, Yang X. The essential roles of CCR7 in epithelial-to-mesenchymal transition induced by hypoxia in epithelial ovarian carcinomas. *Tumour Biol.* 2014;35(12):12293–12298.
45. Basheer HA, Pakanavicius E, Cooper PA, et al. Hypoxia modulates CCR7 expression in head and neck cancers. *Oral Oncol.* 2018;80:64–73.
46. Xu Z, Zhu C, Chen C, et al. CCL19 suppresses angiogenesis through promoting miR-206 and inhibiting Met/ERK/Elk-1/HIF-1alpha/VEGF-A pathway in colorectal cancer. *Cell Death Dis.* 2018;9(10):974.

Tables

Table 1

prognosis significance evaluation for patients in HCC in term of expression of *CCRs*.

Gene expression	Patients (n=212)	RFS						OS			
		No. of event	MRT (months)	Crude HR (95% CI)	Crude *P*	Adjusted HR (95% CI)	Adjusted *P* £	No. of event	MST (months)	Crude HR (95% CI)	Crude *P*
CCR1											
Low	106	62	38	1		1		46	NA	1	
High	106	54	52	0.827(0.574-1.191)	0.307	0.763(0.525-1.107)	0.154	36	NA	0.747(0.483-1.156)	0.189
CCR2											
Low	106	61	42	1		1		44	NA	1	
High	106	55	47	0.849(0.590-1.223)	0.379	0.872(0.603-1.263)	0.470	38	NA	0.787(0.509-1.214)	0.277
CCR3											
Low	106	63	36	1		1		47	NA	1	
High	106	53	55	0.810(0.562-1.168)	0.257	0.90(0.634-1.335)	0.661	35	NA	0.738(0.476-1.143)	0.172
CCR4											
Low	106	63	33	1		1		44	NA	1	
High	106	53	54	0.727(0.505-1.049)	0.086	0.713(0.492-1.034)	0.074	38	NA	0.802(0.519-1.238)	0.317
CCR5											
Low	106	64	29	1		1		48	61	1	
High	106	52	58	0.686(0.476-0.991)	0.043	0.703(0.484-1.022)	0.065	34	NA	0.602(0.388-0.935)	0.022
CCR6											
Low	106	54	52	1		1		36	NA	1	
High	106	62	36	1.241(0.861-1.787)	0.245	1.165(0.806-1.684)	0.416	46	NA	1.359(0.878-2.102)	0.167
CCR7											
Low	106	63	29	1		1		48	NA	1	
High	106	53	53	0.733(0.508-1.056)	0.094	0.824(0.568-1.194)	0.306	34	NA	0.599(0.386-0.930)	0.021
CCR8											
Low	106	53	52	1		1		39	NA	1	
High	106	63	44	1.200(0.832-1.731)	0.327	1.062(0.731-1.544)	0.751	43	NA	1.117(0.724-1.724)	0.616
CCR9											
Low	106	60	44	1		1		46	NA	1	
High	106	56	47	0.811(0.612-1.269)	0.496	0.944(0.651-1.369)	0.763	36	NA	0.765(0.495-1.184)	0.228
CCR10											
Low	106	60	41	1		1		44	NA	1	
High	106	56	52	0.928(0.644-1.336)	0.687	0.885(0.610-1.283)	0.519	38	NA	0.873(0.565-1.348)	0.538

Notes: £ in RFS of patients in HCC adjusted for tumor size, gender, TNM stage and BCLC stage; § in OS of patients in HCC adjusted for tumor size, cirrhosis, BCLC stage, TNM stage and AFP.

Abbreviation: CCR, C-C chemokine receptor; RFS, recurrence-free survival; OS, overall survival; NO, number; MRT, median recurrence time; HR, hazard ratio; CI, confidence interval; MST, median survival time.

Table 2

Joint effects analysis of *CCR5*, *CCR6* and *CCR9* in GSE14520.

Group	*CCR1*	*CCR5*	*CCR7*	Patients	NO. of event	MST(Months)	Crude HR (95% CI)	Crude P	Adjusted HR (95% CI)	Adjusted P δ
A	Low	Low		67	31	61	1		1	
B	Low	High		78	32	NA	0.777(0.474-1.274)		0.920(0.547-1.547)	
	High	Low								
C	High	High		67	19	NA	0.518(0.293-0.918)	0.074	0.445(0.245-0.808)	0.008
	Low		Low	66	34	47	1		1	
	Low		High	80	26	NA	0.526(0.315-0.877)		0.437(0.255-0.748)	
	High		Low							
	High		High	66	22	NA	0.541(0.315-0.926)	0.017	0.491(0.285-0.846)	0.010
a		Low	Low	72	35	53	1		1	
b		Low	High	68	26	NA	0.659(0.396-1.095)		0.588(0.350-0.988)	
		High	Low							
c		High	High	72	21	NA	0.468(0.272-0.805)	0.017	0.473(0.271-0.824)	0.008
1	Low	Low	Low	51	26	47	1		1	
2	Low	Low	High	113	42	NA	0.592(0.363-0.967)		0.586(0.352-0.976)	
	High	Low	Low							
	Low	High	Low							
	Low	High	High							
	High	High	Low							
	High	Low	High							
3	High	High	High	48	14	NA	0.450(0.235-0.862)	0.027	0.450(0.233-0.869)	0.017

Notes: δ in OS of patients in HCC adjusted for tumor size, cirrhosis, BCLC stage, TNM stage and AFP.

Abbreviation: CCR, C-C chemokine receptor; NO, number; MST, median survival time; HR, hazard ratio; CI, confidence interval.

Table 3

CCR1,5,7 were associated with OS in HCC.

Gene expression	Patients (n=25)	OS			
		NO. of event	MST (months)	Crude HR (95% CI)	P
CCR1					
Low	12	6	19	1	
High	13	7	31	0.258(0.061-1.080)	0.045
CCR2					
Low	12	6	21	1	
High	13	7	31	0.184(0.043-0796)	0.013
CCR3					
Low	12	47	NA	1	
High	13	35	NA	0.253(0.067-0.946)	0.029

Abbreviation: CCR, C-C chemokine receptor; OS, overall survival; NO, number; HR, hazard ratio; CI, confidence interval; MST, median survival time.

Figures

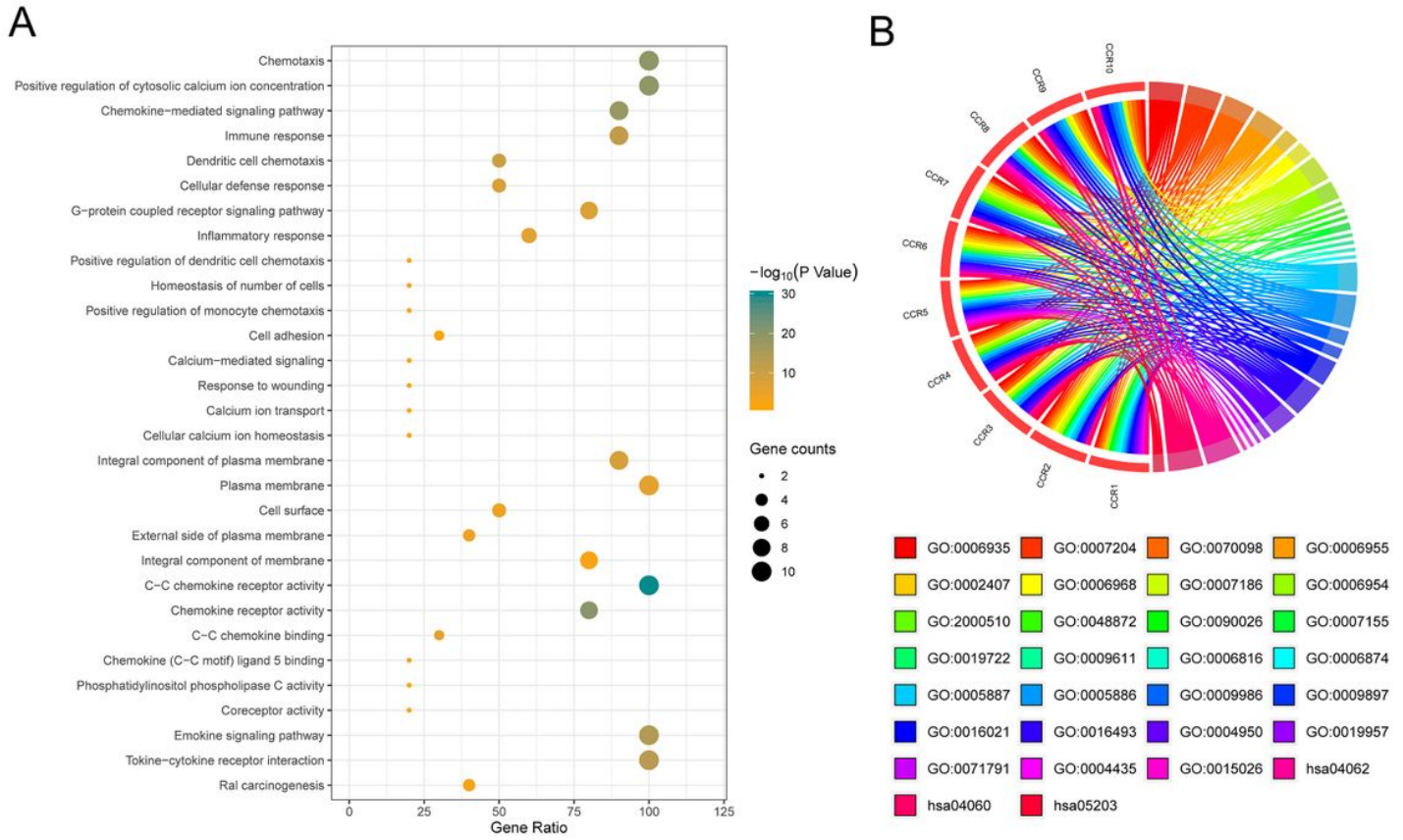

Figure 1

Bioinformatics-based results from DAVID. A, the pathways, molecular functions, biological processes, and cellular components in which CCRs are enriched; B, details of CCRs corresponding to specific pathways, molecular functions, biological processes and cellular components.

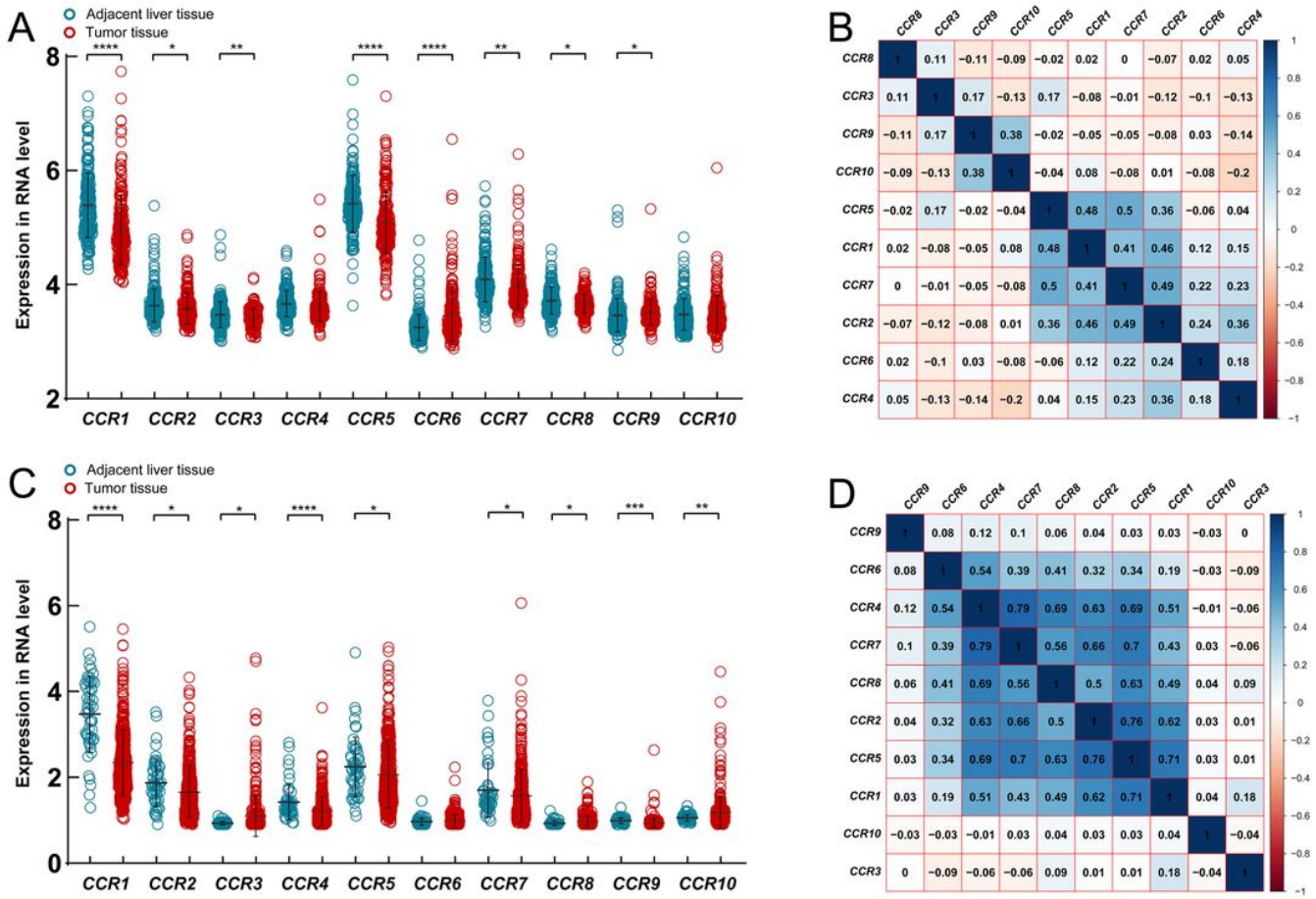

Figure 2

Expression of CCRs in HCC and para-carcinoma tissues. A, expression level of CCRs between HCC and para-carcinoma tissues in GSE14520; B, Matrix graphs of Pearson correlations for CCRs in GSE14520; C, expression level of CCRs between HCC and para-carcinoma tissues in TCGA database; B, Matrix graphs of Pearson correlations for CCRs in TCGA database.

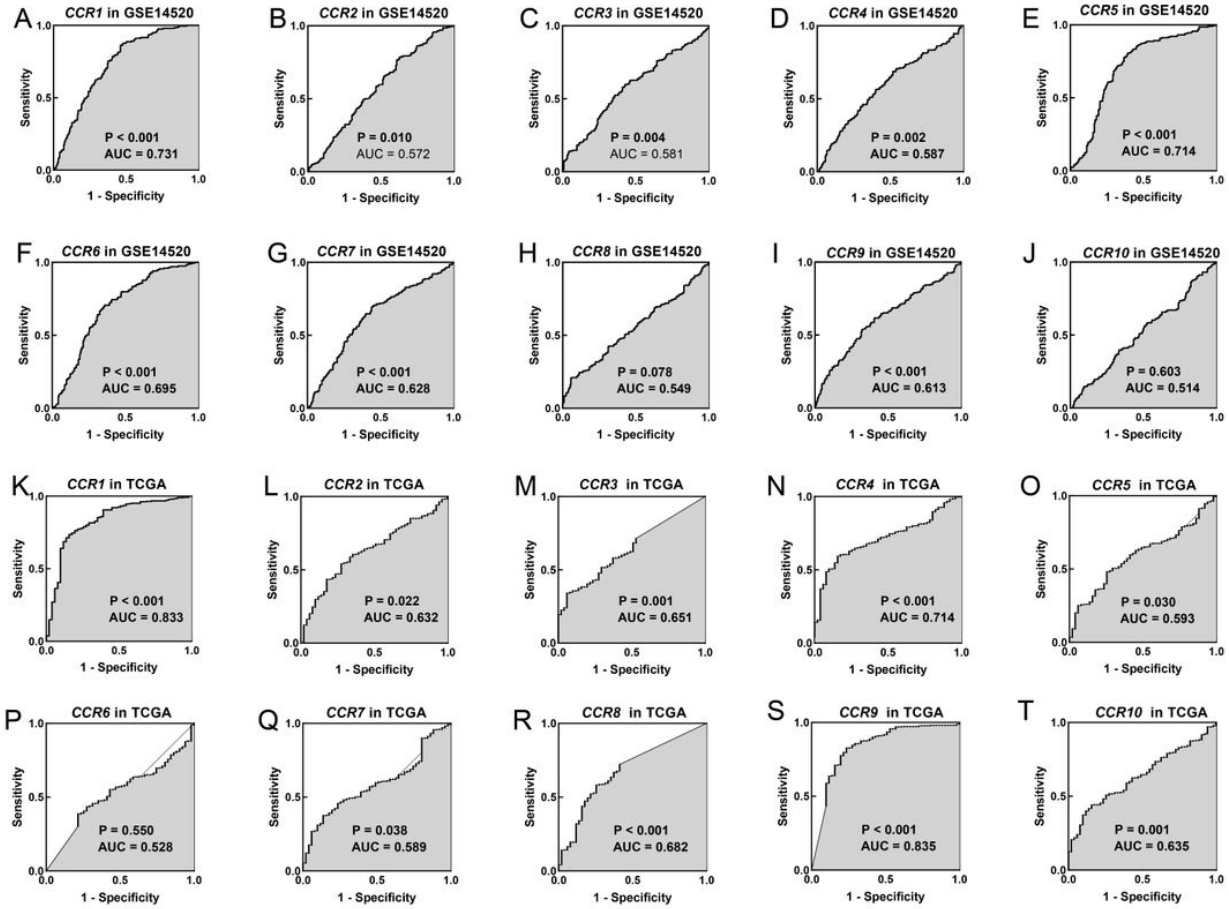

Figure 3

ROC curves of CCRs in GSE14520 and TCGA database. A, CCR1 in GSE14520; B, CCR2 in GSE14520; C, CCR3 in GSE14520; D, CCR4 in GSE14520; E, CCR5 in GSE14520; F, CCR6 in GSE14520; G, CCR7 in GSE14520; H, CCR8 in GSE14520; I, CCR9 in GSE14520; J, CCR10 in GSE14520; K, CCR1 in TCGA; L, CCR2 in TCGA; M, CCR3 in TCGA; N, CCR4 in TCGA; O, CCR5 in TCGA; P, CCR6 in TCGA; Q, CCR7 in TCGA; R, CCR8 in TCGA; S, CCR9 in TCGA; T, CCR10 in TCGA.

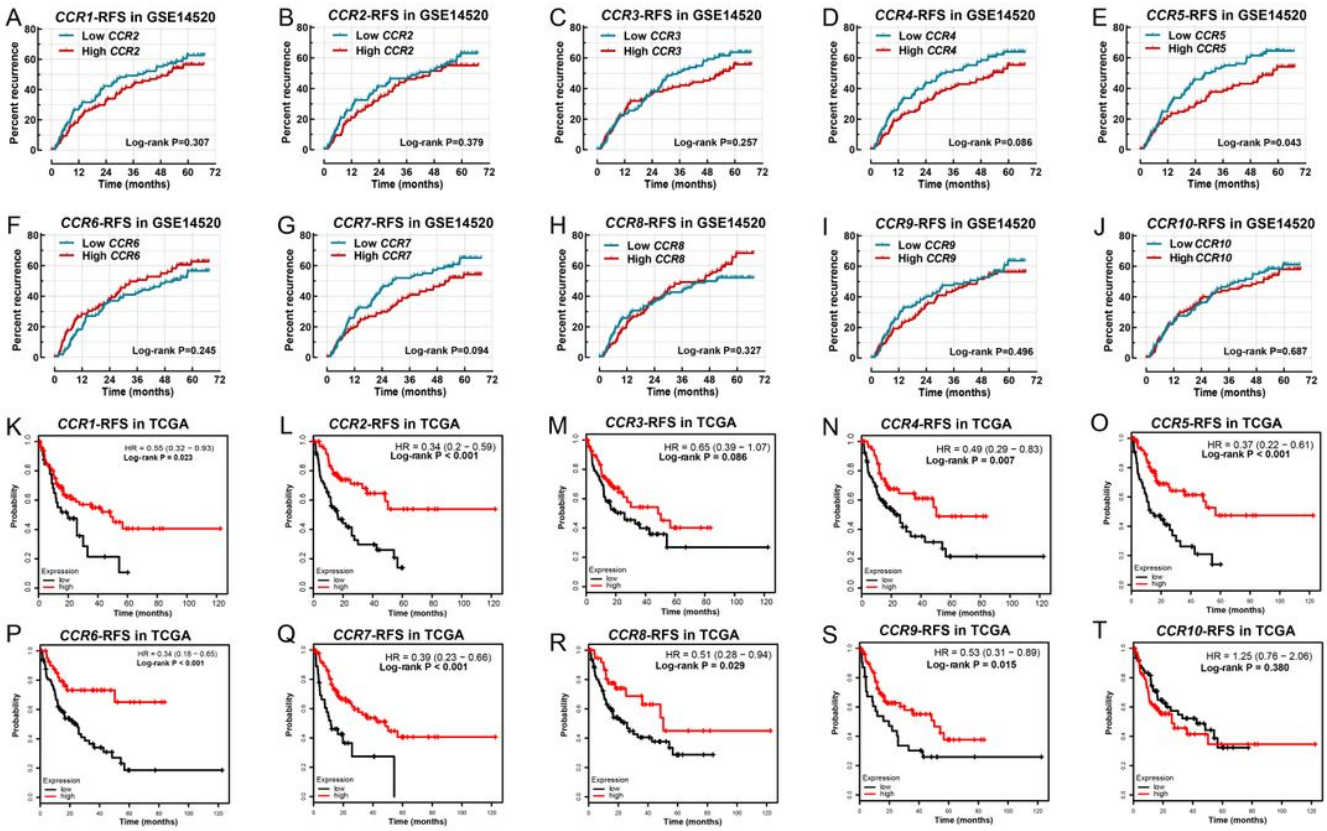

Figure 4

Survival analysis for RFS in GSE14520 and TCGA database. A, CCR1 in GSE14520; B, CCR2 in GSE14520; C, CCR3 in GSE14520; D, CCR4 in GSE14520; E, CCR5 in GSE14520; F, CCR6 in GSE14520; G, CCR7 in GSE14520; H, CCR8 in GSE14520; I, CCR9 in GSE14520; J, CCR10 in GSE14520; K, CCR1 in TCGA; L, CCR2 in TCGA; M, CCR3 in TCGA; N, CCR4 in TCGA; O, CCR5 in TCGA; P, CCR6 in TCGA; Q, CCR7 in TCGA; R, CCR8 in TCGA; S, CCR9 in TCGA; T, CCR10 in TCGA.

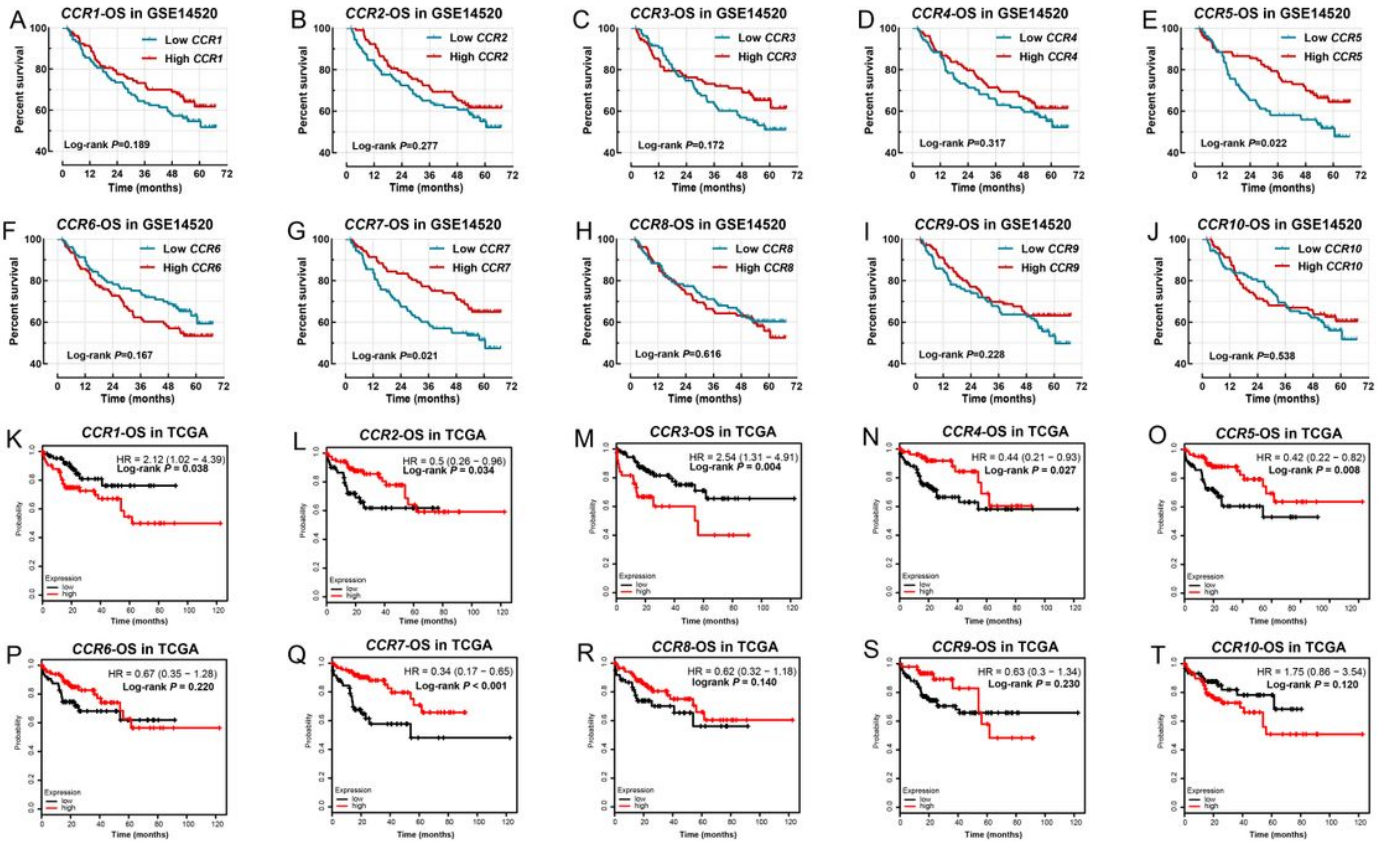

Figure 5

Survival analysis for OS in GSE14520 and TCGA database. A, CCR1 in GSE14520; B, CCR2 in GSE14520; C, CCR3 in GSE14520; D, CCR4 in GSE14520; E, CCR5 in GSE14520; F, CCR6 in GSE14520; G, CCR7 in GSE14520; H, CCR8 in GSE14520; I, CCR9 in GSE14520; J, CCR10 in GSE14520; K, CCR1 in TCGA; L, CCR2 in TCGA; M, CCR3 in TCGA; N, CCR4 in TCGA; O, CCR5 in TCGA; P, CCR6 in TCGA; Q, CCR7 in TCGA; R, CCR8 in TCGA; S, CCR9 in TCGA; T, CCR10 in TCGA.

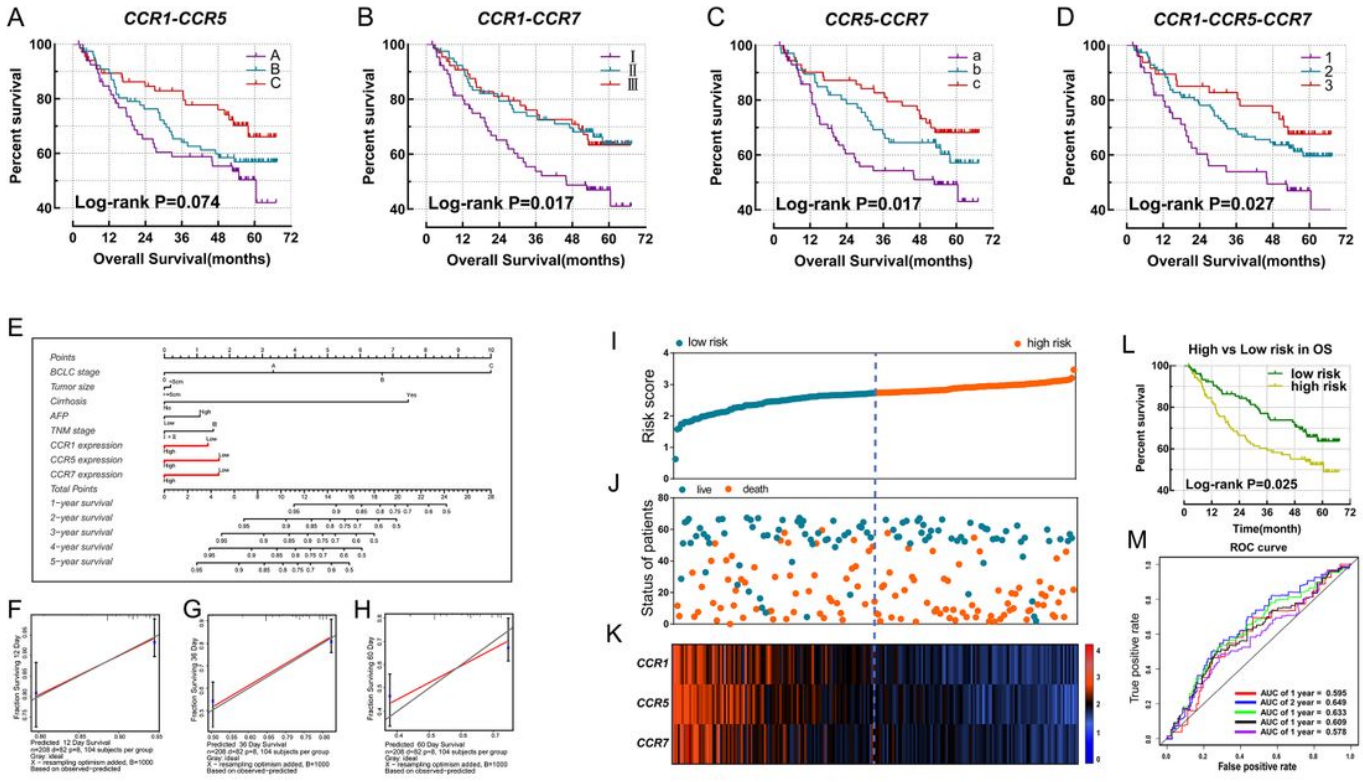

Figure 6

Nomogram and the prognostic signature constructed in GSE14520 in term of CCR1, CCR5 and CCR7. A-D, combined effect survival analysis for OS on the basis of CCR1, CCR5 and CCR7; E, Nomogram; F-H, verification model for nomogram in 1-, 2- and 3-year OS respectively; I, risk score plot; J, survival status scatter plot; K, heat map of the levels of expression of CCR1, CCR5 and CCR7 in low- and high-risk groups; L, Kaplan-Meier curves for low- and high-risk groups; M, Receiver operating characteristic curve for predicting 1-, 2- and 3-year survival in HCC patients by risk score.

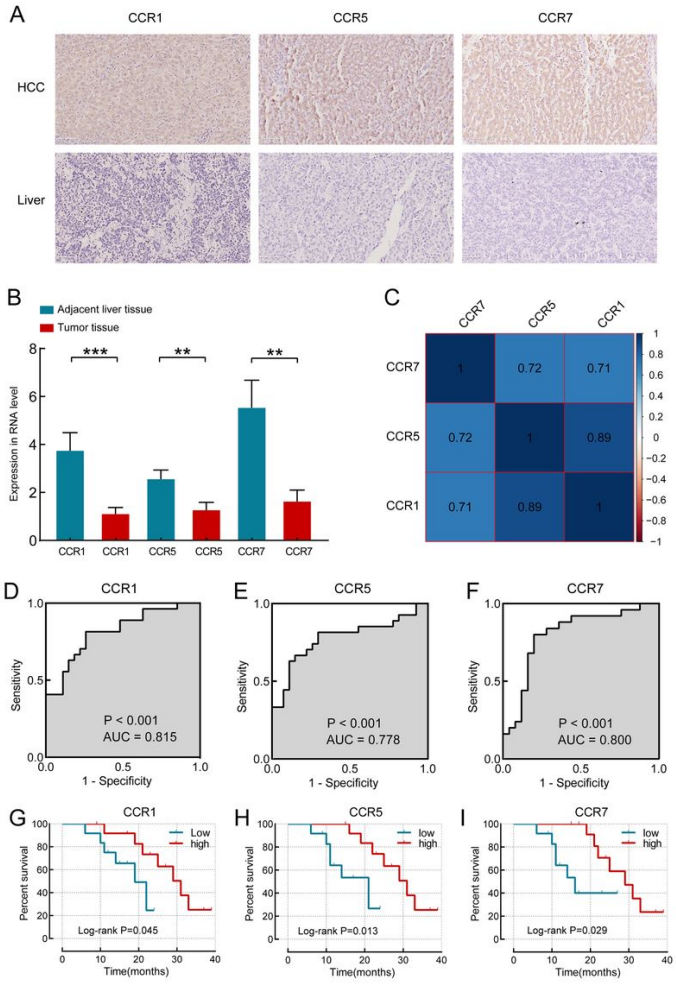

Figure 7

Validation of CCR1, CCR5 and CCR7 in Guangxi cohort. A, Expression of CCR1, CCR5 and CCR7 in HCC and para-carcinoma live tissues detected with IHC assay; A, Expression of CCR1, CCR5 and CCR7 in HCC and para-carcinoma live tissues detected with qPCR assay; C, Matrix graphs of Pearson correlations for CCR1, CCR5 and CCR7; D-F, ROC curves for CCR1, CCR5 and CCR7; G-I, survival analysis for OS in terms of CCR1, CCR5 and CCR7; ** P<0.01; *** P<0.001.

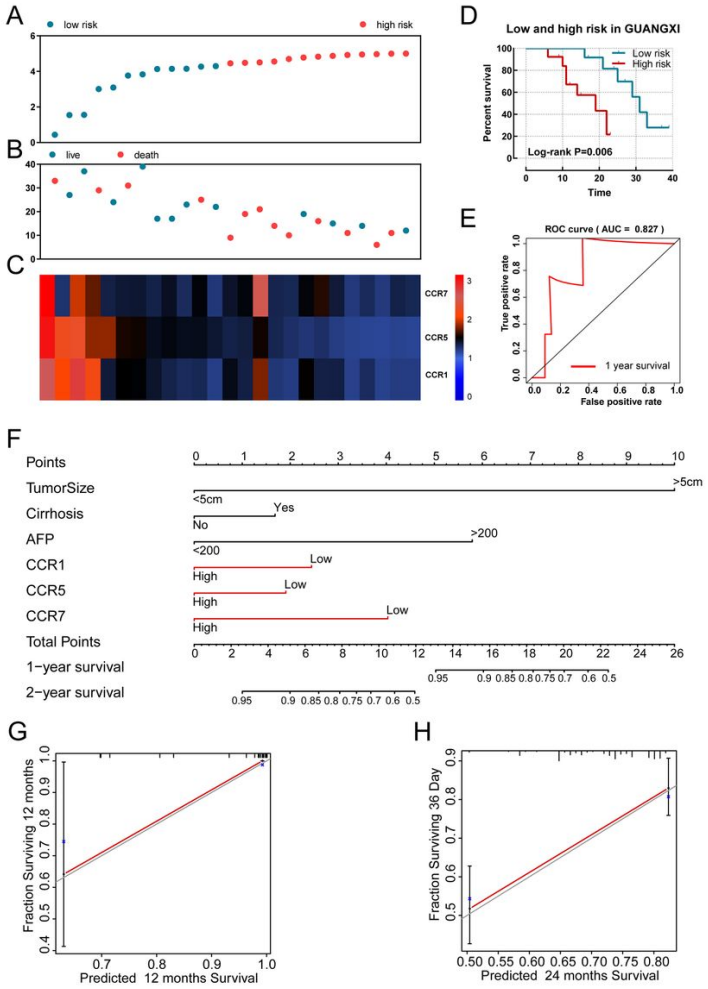

Figure 8

Nomogram and the prognostic signature constructed in Guangxi cohort in term of CCR1, CCR5 and CCR7. A, risk score plot; B, survival status scatter plot; C, heat map of the levels of expression of CCR1, CCR5 and CCR7 in low- and high-risk groups; D, Kaplan-Meier curves for low- and high-risk groups; E, Receiver operating characteristic curve for predicting 1- or 2-year survival in HCC patients by risk score. E, Nomogram; F and G, verification model for nomogram in 1- and 2-year OS respectively;

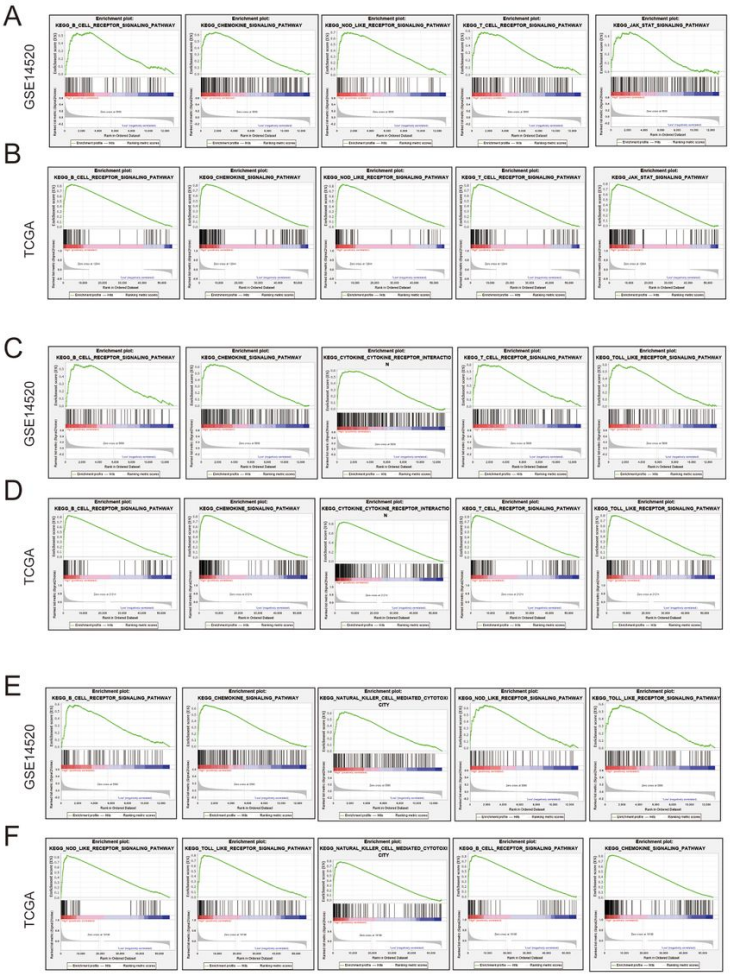

Figure 9

GSEA in terms of CCR1, CCR5 and CCR7 based on C2 curated gene sets. A, Venn diagram for GSEA results of CCR1 in TCGA and GSE14520; B, representative result of GSEA results of CCR1 in GSE14520; C, representative result of GSEA results of CCR1 in TCGA; D, Venn diagram for GSEA results of CCR5 in TCGA and GSE14520; E, representative result of GSEA results of CCR5 in GSE14520; F, representative result of GSEA results of CCR5 in TCGA; G, Venn diagram for GSEA results of CCR7 in TCGA and GSE14520; H, representative result of GSEA results of CCR7 in GSE14520; I, representative result of GSEA results of CCR7 in TCGA.

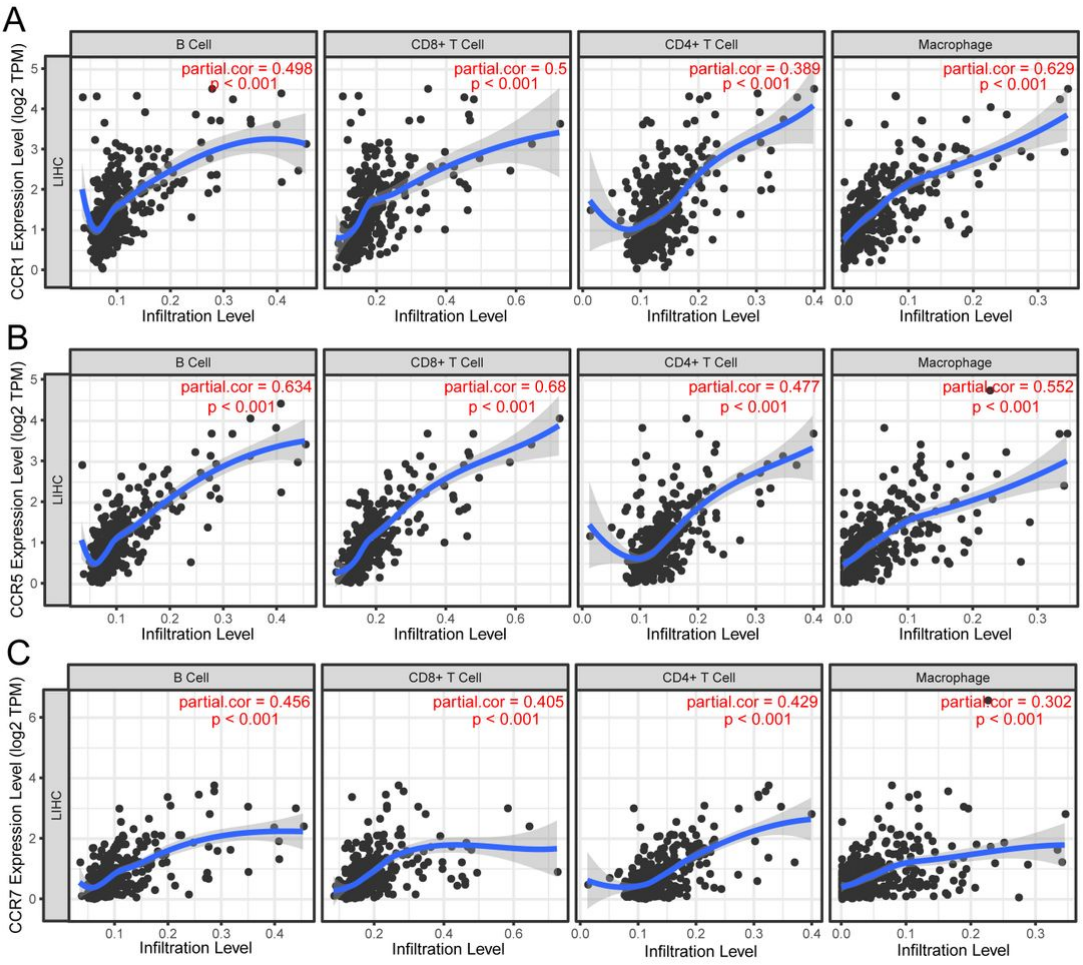

Figure 10

Correlation between CCRs expression and tumor-infiltrating immune cells. A, Scatter plot in terms of CCR1 expression and tumor-infiltrating immune cells; B, Scatter plot in terms of CCR5 expression and tumor-infiltrating immune cells; C, Scatter plot in terms of CCR7 expression and tumor-infiltrating immune cells.

Supplementary Files

This is a list of supplementary files associated with this preprint. Click to download.

- TableS1.docx
- TableS2.docx
- TableS3.docx